2

Solvation: A Molecular Dynamics Study of a Dipeptide in Water

MARTIN KARPLUS
Department of Chemistry, Harvard University, Cambridge, MA 02138

PETER J. ROSSKY
Department of Chemistry, University of Texas, Austin, TX 78712

Water has an essential role in living systems and is ultimately involved in the structure and function of biological polymers such as proteins. However, in this contribution we shall focus primarily not on what the water does for the biopolymer but rather on the effects that the biopolymer has on the water that interacts with it. Of interest are alterations in the structural, energetic, and dynamic properties of the water molecules. Studies of the rotational mobility of water molecules at protein surfaces have been interpreted by dividing the solvent molecules into three groups (1). The most rapidly reorienting group has a characteristic rotational reorientation time (τ_r) of not more than about 10^{-11}s. The next most rapid group exhibits a rotational reorientation time of about 10^{-9}s and has been tentatively identified as the water molecules that are strongly associated with ionic residues. The third group exhibits a τ_r of about 10^{-6}s; these solvent molecules are considered to be essentially irrotationally bound to the macromolecules; an example might be the four waters in the interior of the bovine pancreatic inhibitor. The population exhibiting the fastest times is expected to include molecules which form hydrogen bonds to the peptide backbone and those which are influenced by the presence of nonpolar groups. It is this group which forms the major part of the solvation shell and, therefore, is likely to play the dominant role in the solvent effect on protein properties. Because of the difficulties involved in studies of protein solutions per se, it is of particular interest to investigate systems of small molecules that incorporate functional groups present in proteins.

In this contribution we describe the results of a molecular dynamics simulation of such a molecule, the alanine dipeptide in aqueous solution. In such a simulation, one treats a sample of molecules with fixed volume and an energy and density corresponding to the system of interest. Given the internal and interaction potentials for the molecules in the box, and certain initial conditions for the coordinates and momenta of each particle, one solves the classical equations of motion for all of the particles

0-8412-0559-0/80/47-127-023$05.00/0

to obtain the phase space trajectory of the entire system over a period of time. An initial integration period during which certain properties (e.g., individual particle velocities) are adjusted is used to obtain a system that is equilibrated. After the equilibration period, integration is continued for a length of time sufficient to yield time averages that approximate equilibrium averages. In addition, the time evolution of the particle trajectories can be used to determine time-dependent properties.

We examine structural and dynamic aspects of both the dipeptide solute and the aqueous solvent. For the dipeptide, primary emphasis is placed on the internal motions. The size and dynamical character of fluctuations relative to the average structure are investigated in vacuum and in the presence of solvent. The dipeptide vibrational degrees of freedom have frequencies varying from approximately 50 (dihedral angle torsions) to 3500 cm^{-1} (bond stretching), corresponding to characteristic times in the range of 7×10^{-13} to 1×10^{-14}s. For such a range in characteristic times, a significant variation in solvent effects (e.g., damping of fluctuations) is expected.

The structural and dynamic properties of the aqueous solvent in the region immediately surrounding the dipeptide solute are of special interest. The principal questions which we address are: First, how is the dynamic behavior of the solvent altered by the proximity of the solute? Second, what is the range of influence of the solute; that is, are the effective solvent-solute interactions of sufficiently short range that it is reasonable to regard the water molecules in contact with the polar (peptide) groups as qualitatively different from those in contact with the nonpolar (methyl) substituents? Finally, we investigate the structural origins of observed differences between the dynamic properties of the bulk solvent and that in contact with the solute.

Model

The details of the model used to simulate the dipeptide solution have been presented previously (2); a brief review of the interactions present in the system and the methods used to carry out the simulation is given here. The alanine "dipeptide" solute ($CH_3C'ONHCHCH_3C'ONHCH_3$), shown in Figure 1, is a neutral molecule terminated by methyl groups, rather than by the carboxylic acid and amino groups of an amino acid. This is an appropriate choice to obtain a system that models an amino acid as part of a polypeptide chain. The structure shown in Figure 1 is the equatorial C_7 conformation (C_7^{eq}) that is the global minimum in the dipeptide potential surface in vacuum and is believed to be the favored conformation in both aqueous and nonaqueous solutions.

The internal degrees of freedom of the dipeptide are governed by a molecular mechanics force field (2) that includes terms

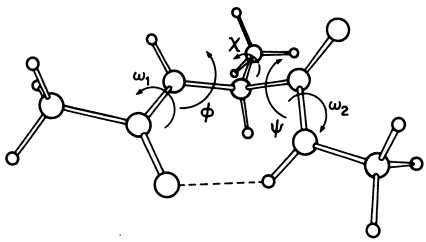

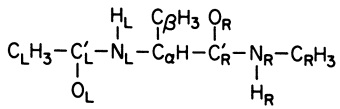

Figure 1. Alanine dipeptide in the equatorial C_7 conformation, $(\phi,\psi) \simeq (-60°, 60°)$. The structure is (left to right) CH_3-$CONHCHCH_3CONHCH_3$; the dashed line represents the internal hydrogen bond.

corresponding to harmonic bonds, anharmonic bond angles, dihedral angle torsions, and nonbonded Lennard-Jones and electrostatic interactions. No dipeptide degrees of freedom are constrained in the simulation. The water molecules are modeled by a modification of the ST2 model of Stillinger and Rahman (3). The model consists of four point charges placed within a single Lennard-Jones sphere centered at the oxygen atom; two positive charges are located at the hydrogen atom positions, and two negative charges are located at positions representing the lone-pair orbitals. The only modification made in the ST2 model is to allow internal flexibility in the water molecules. The intermolecular interactions among the waters are given by pair-wise potentials. For the two molecules W_1 and W_2, we have

$$V_{w_1w_2} = 4\varepsilon_W\left\{\left(\frac{\sigma_W}{r_{0_1 0_2}}\right)^{12} - \left(\frac{\sigma_W}{r_{0_1 0_2}}\right)^{6}\right\} + \sum_{i,j=1}^{4} \frac{q_i^{w_1} q_j^{w_2}}{r_{ij}} S(r_{0_1 0_2}) \qquad (1)$$

where σ_W and ε_W are the parameters characterizing the Lennard-Jones interaction, q_i^W is the ith charge in water molecule W, $r_{0_1 0_2}$ is the intermolecular oxygen-oxygen distance, S(r) is a switching function (3). The interactions between each water molecule and the dipeptide are given by a sum of Lennard-Jones and electrostatic terms of the form

$$V_{WD} = \sum_{\substack{\text{dipeptide} \\ \text{atoms, } \lambda}} \left[4\sqrt{\varepsilon_w \varepsilon_\lambda}\left\{\left(\frac{\bar{\sigma}_\lambda}{r_{0\lambda}}\right)^{12} - \left(\frac{\bar{\sigma}_\lambda}{r_{0\lambda}}\right)^{6}\right\} + \sum_{j=1}^{4} \frac{q_j^W q_\lambda}{r_{j\lambda}}\right] \qquad (2)$$

where $\bar{\sigma}_\lambda = (\sigma_w + \sigma_\lambda)/2$ and $r_{0\lambda}$ is the water oxygen-dipeptide atom distance. For the chosen values (2) of dipeptide-atom Lennard-Jones parameters, σ_λ and ε_λ, and charges, q_λ, the water molecules associated with the solute peptide groups have reasonable energies and geometries. In particular, the optimal association energies (kcal/mol) for the four types of hydrogen bonds in the system in order of increasing strength (the water HOH bond angle is fixed at the tetrahedral angle) are NH ... H_2O (-6.0) < H_2O ... H_2O (-6.8) < C = O ... H_2O (-7.4) < N-H ... O = C (-8.1). The values of the association energies are adjusted to the water-water interaction energy given by the ST2 model so that the hydrogen bond strengths are all similar, in accord with available

calculations and data.

The simulation is carried out on a sample consisting of one dipeptide and 195 water molecules in a cubic box with an edge length of 18.2194 Å; the density of 1.004 g/cm^3 is in accord with experiment. The dipeptide solute is surrounded by approximately two molecular layers of water at all points. After the equilibration, the simulation analyzed in the current work corresponds to 4000 time steps of 3.67 x 10^{-16}s, or 1.5 ps on a molecular time scale. The mean solvent kinetic temperature is 303°K and that of the dipeptide is 298°K.

Solute Properties

During the simulation, the solute remains in the vicinity of the C_7^{eq} minimum. This is not to be interpreted as implying that the C_7^{eq} is the most stable solution structure, because there is a very small probability of observing a large conformational change in such a short time.

To determine the effect of the water on the dipeptide in solution, we did a corresponding simulation of the dipeptide dynamics in the absence of solvent. Neither the average structure nor the magnitude of the local fluctuations of the dipeptide is strongly affected by the solvent environment. The results are summarized in Table I, where we give results for typical bonds, bond angles, and dihedral angles (see Figure 1). With the exception of the fluctuations in the dihedral angles ψ and χ the observed differences are within the statistical error of the calculation.

Correlation Functions. We next consider dynamic correlations of the solute fluctuations. The time correlation function for solute structural fluctuations is defined as

$$C_A(t) = \frac{\langle \Delta A(\tau)\Delta A(t+\tau)\rangle_\tau}{\langle \Delta A^2\rangle} \equiv \frac{\langle \Delta(0)\Delta A(t)\rangle}{\langle \Delta A^2\rangle} \qquad (3)$$

where A is a particular structural parameter (e.g., bond length, dihedral angle), $\Delta A(t) = A(t) - \langle A\rangle$, $\langle \Delta A^2\rangle = \langle (A - \langle A\rangle)^2\rangle$, and the brackets indicate an average over the simulation; in the numerator of eq 3, the average includes all values, τ, in the simulation.

The unperturbed harmonic vibration of an isolated bond of length b would lead to a correlation function, $C_b(t)$, which oscillates without decay for all times. However, shifts in either the frequency or phase of the oscillation results in an eventual decay of $C_b(t)$ to zero after a time when the phase of $\Delta b(t)$ is, on the average, completely random with respect to that of $\Delta b(0)$. Even in an isolated molecule, such a decay can occur due to coupling of the motion of various degrees of freedom with different frequencies, although over long times the correlation function cannot remain zero since there is no dissipation. The change in

Table I

Average Solute Structure

A[a]	<A> vacuum	<A> solution	$\langle\Delta A^2\rangle^{1/2}$ vacuum	$\langle\Delta A^2\rangle^{1/2}$ solution
		Bonds[b]		
C'_L-O_L	1.235	1.237	0.023	0.028
N_L-H_L	0.994	0.997	0.018	0.012
$C_\alpha-C_\beta$	1.544	1.542	0.041	0.035
N_R-C_R	1.461	1.459	0.034	0.032
		Bond Angles[b]		
$C_L-C'_L-O_L$	122.31	121.89	3.30	3.23
$N_L-C_\alpha-C_R$	114.73	114.46	4.25	3.93
$N_L-C_\alpha-C_\beta$	107.71	108.15	3.51	3.85
$C'_R-N_R-H_R$	120.97	120.68	3.97	4.29
		Dihedral Angles[b,c]		
ϕ	-67.21	-63.96	9.67	7.83
ψ	63.45	59.33	11.53	22.57
ω_1	-179.25	-179.67	8.74	9.67
ω_2	-179.68	178.08	14.72	12.39
χ	-59.10	-62.88	9.96	32.25

[a]All structural parameters, A, are defined in Figure 1; <A> = mean value, $\langle\Delta A^2\rangle^{1/2} = \langle(A-\langle A\rangle)^2\rangle^{1/2}$. [b]Bonds in Angstroms, bond angles and dihedral angles in degrees. [c]The vacuum minimum occurs at $\phi = 66.2°$, $\psi = -65.3°$, $\omega_1 = 179.2°$, $\omega_2 = 179.9°$.

the correlation function in solution is determined by the effectiveness of solvent-solute collisions in dissipating the solute's dynamical information. In water, these "collisions" can involve the repulsive forces characteristic of hard sphere-like systems and the strong hydrogen bonding forces; weak attractive van der Waals interactions are expected to have only a small effect. Collisions with solvent are more likely to affect the solute motion if the latter is associated with a small characteristic force constant or if the mass of the solute structural component involved is small; also, damping is generally more effective for motions involving structural components of increased spatial dimensions. In the current study, a comparison of different dipeptide structural motions shows the expected qualitative differences in behavior.

We illustrate the results by presenting the correlation functions for (see Figure 1) a typical bond (C_α-C_β) in Figure 2, a typical bond angle (N_L-C_α-C_R') in Figure 3, and the dihedral angle χ in Figure 4. In each figure, we show the result obtained in solution at the top and that obtained in vacuum at the bottom. The spectral density as a function of frequency ω corresponding to $C_A(t)$ is

$$\tilde{C}_A(\omega) = \int_o^\infty dt\ \cos(\omega t) C_A(t) \qquad (4)$$

The limited knowledge of $C_A(t)$ forces us to truncate the time integral at t_{max}, rather than at infinite time; the calculated spectral density function is shown in an inset in each case (the amplitudes are in arbitrary units). Negative values of $\tilde{C}_A(\omega)$ result from the finite upper limit on the integration.

On the picosecond time scale considered, no significant damping is seen in the oscillatory correlation functions describing the high-frequency ($\omega \gtrsim 300\ cm^{-1}$) bond-length stretching and bond-angle bending modes. It is clear that for these high-frequency motions, the behavior of the time correlation functions is very similar in solution as compared to vacuum, and that in both environments there is no evidence for a significant zero-frequency component in the spectral density. The latter is expected if the correlation function contains a decaying component.

Clear evidence of solvent damping is found for the torsional angle χ (Fig. 4) for which the vacuum motion can be seen to involve principally a single frequency. During the current simulation, the motion involves only libration and not overall reorientation of the methyl group. By comparison with the result in the absence of solvent, it can be seen that the solvent is effective in damping the oscillatory motion of the methyl group. The behavior is manifest by the appearance of a low-frequency component in the spectral density, $\tilde{C}_\chi(\omega)$. The short-time behavior of the solution correlation function ($t \lesssim 0.1$ ps) is roughly consistent with underdamped motion calculated from a Langevin equation,

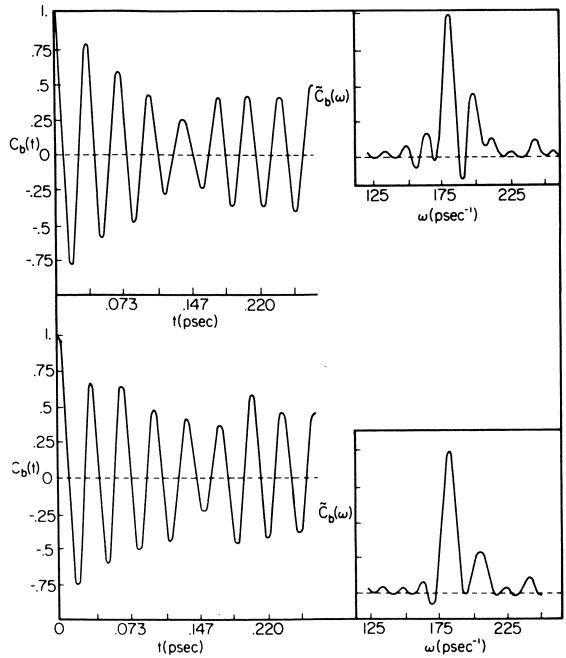

Figure 2. Time correlation function and spectral density for fluctuations in the bond length, C_α—C_β (Figure 1). Top: in solution; bottom: under vacuum.

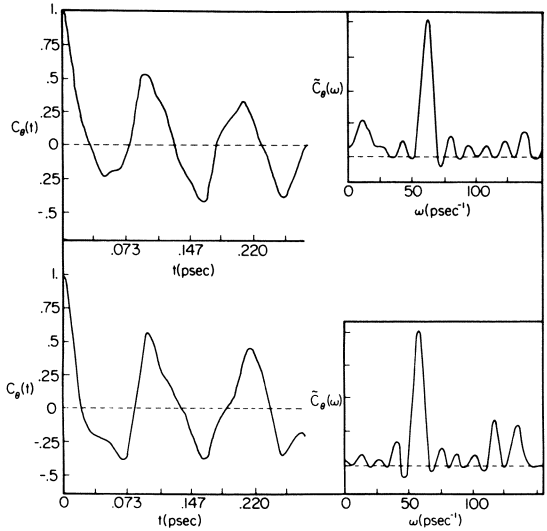

Figure 3. Time correlation function and spectral density for fluctuations in the bond angle, N_L—C_α—C_R' (Figure 1); Top: in solution; bottom: under vacuum.

$$I \frac{d^2\chi}{dt^2} + I\omega_0^2 \chi + f \frac{d\chi}{dt} = F_R(t) \qquad (5)$$

where I is the moment of inertia of the methyl group (3 amu Å^2), ω_o is the harmonic vacuum frequency (35 ps^{-1}; see Fig. 4), f is a frictional coefficient, and $F_R(t)$ is a white noise random force. The time correlation function calculated for motion governed by the Langevin equation is shown as a dotted line at the top in Figure 4. It is in reasonable agreement for short times with the correlation function $C_\chi(t)$ found in solution when the characteristic time, 2I/f, is chosen to be 0.05 ps; the corresponding spectral density is shown dotted in the inset. It is evident that for times greater than about 0.15 ps the correlation functions are not in agreement. This discrepancy is reflected in the spectral density; the Langevin equation predicts only a single peak in $\tilde{C}_\chi(\omega)$ ($\omega \sim 25$ ps^{-1}) and not two. We note that the initial decay of $C_\chi(t)$ corresponds to an apparent solvent drag which is much smaller than hydrodynamic estimates that assume stick boundary conditions. For example, treating the methyl group as a sphere of radius a = 2.5 Å (the van der Waals radius) to obtain the frictional coefficient, f, $f = 8\pi\eta a^3$ (η is the shear viscosity, 0.01 P) we find 2I/f equal to 0.0003 ps, i.e., about 150 times smaller than that observed. In this sense, the observed drag is nearer to the hydrodynamic slip boundary condition limit; the exact slip limit for a sphere corresponds to f = 0 and an infinite relaxation time. The relatively long relaxation time is consistent with the results of experimental studies of the rotational motion of small nonassociated molecules (4).

Structure and Dynamics of the Solvent

The structural and dynamic properties of the water in the immediate vicinity of the dipeptide, the so-called solvation "shell", can best be characterized by dividing the water molecules included in the simulation into the groups according to whether they are near solute polar groups (polar), near nonpolar groups (nonpolar), or outside of the first solvation layer (bulk). This division is shown schematically in Figure 5. The central blank area immediately surrounding the solute corresponds to the region from which the centers (i.e., the oxygen atoms) of the solvent molecules are excluded by the solute. The outer square corresponds to the wall of the box which encloses the centers of all 195 water molecules. Individual water molecules are classified into groups according to the average distance between their oxygen atom and each of the amide H and carbonyl O atoms of the two peptide links and three methyl carbon atoms; the average is taken over the time of the stimulation. Each of the 195 water molecules is assigned to one of the three solvent classes; polar if the mean distance to any of the four polar atoms is less than

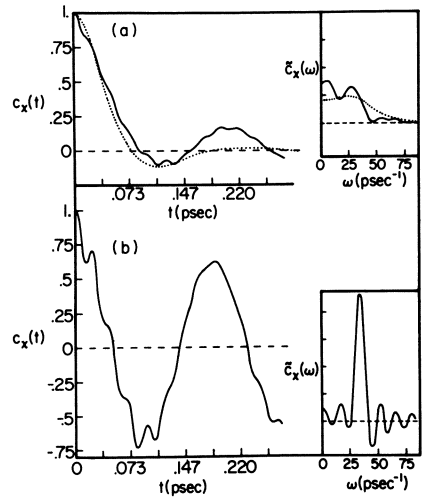

Figure 4. Time correlation function and spectral density for fluctuations in the dihedral angle, χ (Figure 1). Top: in solution; bottom: under vacuum. The functions shown dotted at the top are obtained from a Langevin equation (see text).

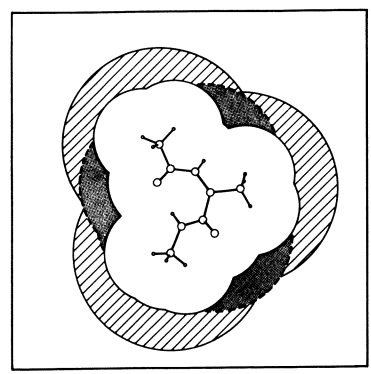

Figure 5. Schematic of the solvation regions defined in the text; "polar," dotted; "nonpolar," cross-hatched; "bulk," within outer square and outside shaded regions.

4 Å, nonpolar if the mean distance is greater than 4 Å to a polar atom but less than 5 Å to a methyl carbon, and "bulk" if neither preceding criterion is met. The division into solvent groups results in the assignment of 14 molecules as "polar", 20 as "nonpolar", and the remaining 161 molecules as "bulk". Although only a fraction of the molecules in the polar group participates in strong bonds with the dipeptide, their proximity to the polar atoms leads to a significant interaction energy with the peptide groups.

One quantity of interest that is obtained from the simulation is the pair radial distribution function, g(r). In Figure 6, we show the water molecule oxygen-oxygen pair distribution function, $g_{OO}(r)$, obtained from the current simulation including all solvent pairs. The results is the same as that obtained from simulations of bulk water (3), within the statistical accuracy of the calculation. We note that the function $g_{OO}(r)$ is characterized by narrow peaks and troughs, a result of the hydrogen-bonded structure. The first peak occurs at 2.85 Å corresponding to the energy minimum of the O—H...O hydrogen bond. The average distribution of water oxygen atoms around the methyl group carbon atoms, $g_{OO}(r)$, is shown in Figure 7; the result is the average over the three solute methyl groups. In contrast to Figure 6, the first peak is broad. The center of the peak occurs at about 3.7 Å, comparable to the average water molecule, methyl group van der Waals contact distance of about 3.8 Å. Since water molecules can make contact with the methyl groups only within a restricted solid angle around the carbon atom (due to the presence of the remainder of the solute attached to the methyl group), the height of the first peak in $g_{OC}(r)$ is reduced relative to the value that would be obtained if the group were completely exposed to solvent (e.g., as in a methane molecule in solution). The breadth and radial position of the first peak are comparable to that found in studies on argon-like systems (5); that is, the first peak occurs at nearly the van der Waals contact distance and is relatively broader than that in $g_{OO}(r)$ for water, particularly on the larger r side of the peak. In argon, as for $g_{OC}(r)$, the structure is determined by the repulsive core of the Lennard-Jones spheres, rather than by the strong attractive hydrogen bond forces characterizing pure water.

The translational and rotational mobility of the solvent molecules can be characterized by time correlation functions. The time correlation functions for rotational motion are

$$C_\ell(t) = \lim_{t'\to\infty} \frac{1}{t'} \int_0^{t'} d\tau \, P_\ell(\hat{\mu}(\tau) \cdot \hat{\mu}(t+\tau)) = \langle P_\ell(\hat{\mu}(0) \cdot \hat{\mu}(t)) \rangle \equiv \langle P_\ell(\cos\theta(t)) \rangle \quad (6)$$

(where $P_\ell(x)$ is the Legendre polynomial of order ℓ) measure the average reorientation rate of the molecular dipole direction, given at time t by the unit vector, $\hat{\mu}(t)$. As in Equation 3, the averages in Equation 6 are evaluated using all pairs of configurations separated by a time t during the simulation of finite length, t'. In particular, we have

$$C_1(t) = \langle \cos \theta \rangle \tag{7}$$

and

$$C_2(t) = \langle (3 \cos^2 \theta - 1)/2 \rangle \tag{8}$$

These correlation functions decay to zero as the molecular orientation becomes randomized with respect to its initial value; $C_2(t)$ typically decays more quickly than $C_1(t)$. The calculated results for $C_1(t)$ (Equation 7) are shown in Figure 8 for the different groups of water molecules. The initial rapid decay of the correlation function during the first 0.05 ps corresponds to overall molecular oscillation (libration) with a loss of phase memory, but without significant net reorientation. In this short time period, the three groups appear to behave similarly. However, for longer times, there are differences in the decay rates of $C_1(t)$. The molecules in the polar class reorient at a rate similar to that exhibited by the bulk class, while those in the nonpolar class reorient more slowly. We can obtain an easily comparable measure of the decay rates for each solvent class from the computed functions by carrying out a least-squares fit to a single exponential; for this fit, we consider the period from 0.25 to 0.6 ps. The narrow solid line drawn through each curve in Figure 8 corresponds to such an exponential fit. The relaxation times obtained in this way, denoted τ_1, are shown in Table II, which also includes values for τ_2 and for the translational diffusion constant D of the various groups of water molecules. From Table II, it is clear that, both for translational and rotational motion, the water molecules in the neighborhood of the methyl groups (nonpolar) are less free (small D, larger τ_1 and τ_2) than the water molecules associated with C=O or N–H groups (polar) or the "bulk" water. Experimental estimates for reorientation rates, primarily from NMR, suggest a factor of 2 to 3 for water molecules in the neighborhood of nonpolar solutes (6).

To determine the origin of the differences among the groups of water molecules, we examine certain time-averaged structural and energetic properties. We consider first some average properties related to the bonding energetics. Of interest are the strengths of the hydrogen bonds involving the different solvent species, the total interaction energies in the presence and absence of the solute, and the number of hydrogen bonds formed by each molecule. Figure 9 shows the calculated distributions of water-water pair interaction energies. In the figure, the

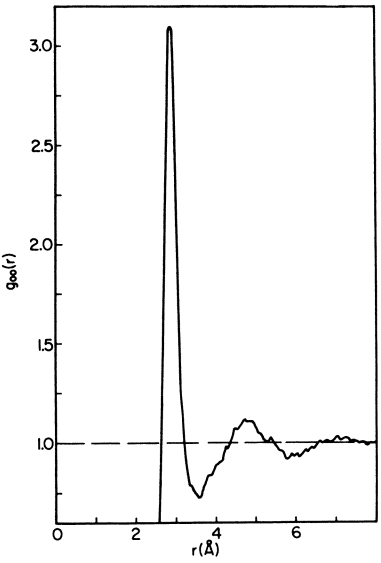

Figure 6. Water oxygen–oxygen pair correlation function computed, including all water molecular pairs

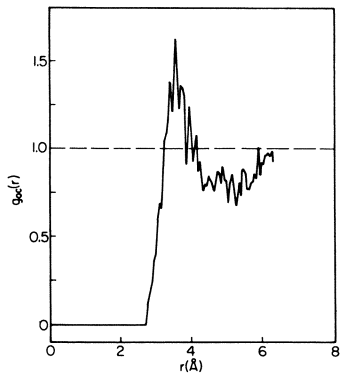

Figure 7. Water oxygen–methyl group carbon pair distribution, averaged over the three solute methyl groups

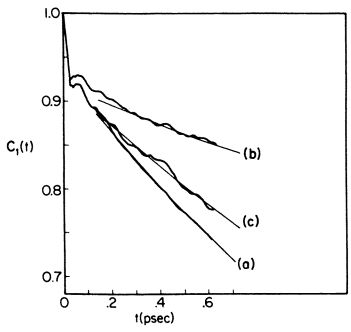

Figure 8. Rotational reorientation of water molecular dipole direction for $l = 1$ *(Equation 7); (a) "bulk"; (b) "nonpolar"; (c) "polar," as defined in text.*

relative origins of the curves labeled (b) and (c) are shifted upward by 0.008 and 0.004, respectively; the particular values given on the ordinate refer to the curve labeled (a). Each curve gives the probability $P(\epsilon)$ of observing a pair of molecules with interaction energy, ϵ, when all pairs within the potential range (8 Å) of each other are included; the curves are individually normalized such that their integral is unity. The three separate distributions correspond to (a) all distinct molecular pairs in the system; (b) all pairs which include at least one molecule in the nonpolar class; and (c) all pairs which include at least one molecule in the polar class. The peak at $\epsilon = 0$ includes the relatively large number of molecular pairs which are well separated in space and therefore have very small average interaction energies; the number of such pairs is finite owing to the finite potential range. The general shape of these curves, including the appearance of a local maximum in the negative energy region, is that expected from studies of pure water (3).

To define hydrogen-bonded water pairs, we use an energy criterion (-3 kcal/mol) in accord with the shape of the distribution in Figure 9; this value corresponds approximately to the position of the local minimum that separates the central peak from the bonding region. However, the precise value is not essential to the interpretation of the results of the simulation.

The strength of intermolecular bonding for each type of solvent is reflected by characteristics of the peak occurring near $\epsilon = -5$ kcal/mol in the curves of Figure 9. It is clear that there are only small differences, if any, in the position of the peak; that of the polar group is at a slightly more positive energy, and that of the nonpolar group at a slightly more negative energy than that of the total system. An alternative comparison is obtained from the calculated mean pair energy, $\bar{\epsilon}$, for bonded pairs ($\epsilon \leq -3$ kcal/mol). The relative values of $\bar{\epsilon}$, which are given in Table III, are in accord with the positions of the peaks in the figure. The shift is much smaller than $k_B T$ (~ 0.6 kcal/mol), indicating that changes in hydrogen bond energies, per se, cannot account for the observed differences in dynamic behavior.

It is important, however, to note that very small changes in the mean bond energy can have significant thermodynamic effects. The bonding region for the nonpolar group (curve (b)) includes contributions from 40 distinct molecular pairs in a typical configuration. Consequently, a shift of only -0.05 kcal/mol in the mean bond energy (Table III) contribute an enthalpy change of -2 kcal/mol. This result suggests that enthalpies of solution are sensitive to small changes in the average bond energies. The total energy of solution from the gas phase obtained from the calculation is -6.72 kcal/mol. This can be thought of as resulting from a cancellation between the change in "nonpolar" water-water bonding (-3.4 kcal/mol), "polar" water-water bonding (+19.32 kcal/mol), and water-solute interaction (-22.64 kcal/mol). Of the latter contribution, -15.82 kcal/mol arises from the "polar" water

Table II

Characteristics of Translational and Rotational Mobility

H_2O class[a]	D, $10^{-5}cm^2/s$	τ_1, ps	τ_2, ps
total	3.24	3.4	1.4
bulk	3.45	2.7	1.1
polar	2.8	3.7	1.8
nonpolar	0.68	8.6	3.1

[a]As defined in the text.

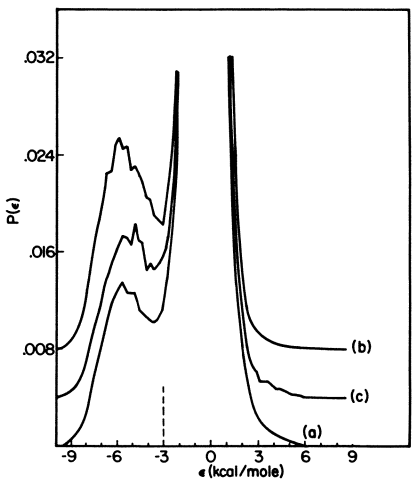

Figure 9. Normalized distributions of pair interaction energies among water molecules; a hydrogen bond is defined by $\epsilon \leq -3$ *kcal/mol, indicated by the vertical mark on the abscissa: (a) all pairs in the system; (b) one of the pair in the "nonpolar" class; (c) one of the pair in the "polar" class. Each curve is integrally normalized to unity.*

Table III

Water-water Hydrogen Bond Energies[a]

class[b]	mean bond energy, $\bar{\epsilon}$
total	-5.25
nonpolar	-5.35
polar	-5.21

[a]Calculated from results shown in Figure 23; a hydrogen bond is defined as $\epsilon \leq -3$ kcal/mol. [b]As defined in the text.

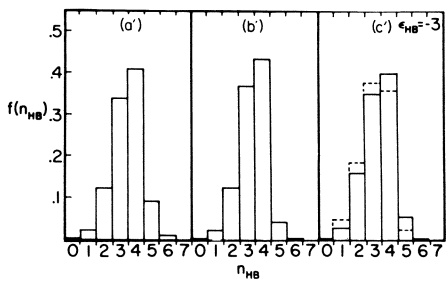

Figure 10. Fraction of water molecules participating in n_{HB} hydrogen bonds, according to the bond definition, ϵ_{HB}. Distribution are: (a') "bulk"; (b') "nonpolar"; (c') "polar". Dashed lines include only water–water bonds; solid lines include also water–dipeptide bonds.

molecules, -3.60 kcal/mol from the "nonpolar" molecules, and 3.22 kcal/mol from the "bulk". Hence, although the long-range interactions are individually small (-0.02 kcal/mol for each "bulk" molecule), they are not insignificant in the total.

We now examine the number of hydrogen bonds formed by a typical water molecule in each of the three groups. Histograms presenting the average fraction, $f(n_{HB})$, of water molecules which participate in n_{HB} hydrogen bonds are shown in Figure 10; the energy criterion is ϵ_{HB} = -3 kcal/mol. It is clear that the distributions are very similar. Thus, a typical water molecule participates in roughly the same number of hydrogen bonds in any of the three environments. For the polar group, we see that the bonds to the dipeptide contribute significantly; they tend to shift the peak in the distribution to higher values of n_{HB} and make the result more similar to that in the bulk than if these bonds are excluded. The average number of hydrogen bonds is 3.45 for bulk, 3.35 for nonpolar, and 3.28 for polar water.

From the distribution functions, the number of molecules in the first water shell around each water molecule is found to be 5.75 (bulk), 4.95 (polar), and 4.70 (nonpolar); that is, the water molecules in the bulk have roughly one more nearest-neighbor water molecule than those in the first solvation shell of the dipeptide. Since the average number of hydrogen bonds formed by molecules in the nonpolar group is essentially equal to that in the bulk, there must be bonding among a significant higher fraction of nearest-neighbor pairs in the former than in the latter. For the solvent molecules near a polar group the average number of neighbors capable of hydrogen bonding is not reduced, since a hydrogen bond to the solute can take the place of that to a water molecule.

The formation of the same number of hydrogen bonds by the water molecules at the surface of a nonpolar solute as by those in bulk water entails significant restrictions on the orientation of the former. From the schematic representation shown in Figure 11, we see that the maximum number of favorable water-water interactions can occur if none of the hydrogen atoms or lone-pair orbitals of the solvent molecule is directed toward the nonpolar group. If θ is the angle between an O-H bond direction (or O-lone pair direction) and the axis defined by the methyl carbon and solvent oxygen, the ideal orientation corresponds to $\theta = 0$. This molecular orientation is typical of crystalline clathrate hydrate compounds. In the simplest picture, optimum solvent hydrogen bonding can be achieved as long as one of the four bonding directions in the water molecule points away from the nonpolar surface. Consequently, we consider the four charges in the model water molecules as equivalent and compute a distribution for their orientations. To examine the calculated distribution of orientations, the angle θ is redefined as the angle formed by any one of the four charges of the solvent molecule, the solvent-center of mass, and the methyl carbon atom. The lower curve in Figure 12 shows the calculated

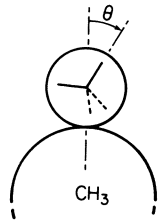

Figure 11. Schematic of water molecule orientation near a nonpolar (—CH_3) group.

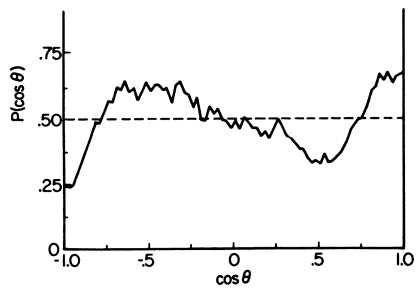

Figure 12. Distribution of orientations of water molecules near methyl groups (lower curve); θ as shown in Figure 11. All four solvent charges are included in the distribution, as described in the text.

distribution of charge directions, averaged over the "nonpolar" solvent neighbors of the three methyl groups. The expected orientational bias of charges away from the nonpolar group is seen; that is, the distribution peaks around $\theta = 0$ ($\cos\theta = 1$) and has its minimum at $\theta = 180°$ ($\cos\theta = -1$). The probability of orientations with one charge directed away from the methyl group (i.e., at $\theta = 0$) is approximately three times that found with one toward it (i.e., at $\theta = 180°$). There is a broad secondary peak in the region $-0.1 > \langle\cos\theta\rangle > -0.8$. This corresponds to the maximum at $\theta = 0$ and is expected from the three other charges at $\cos\theta = -1/3$ for four tetrahedrally arranged charges; there is a corresponding minimum in the neighborhood of $\cos\theta = 1/3$. It is evident from the width of these maxima and minima that there is a significant dispersion in the orientations found in solution; contributions from nonoptimal orientations (e.g., that involving the two OH bonds bridging the methyl group) are clearly important.

In summary, the present study of the kinetic and structural properties of the aqueous solvent surrounding an alanine dipeptide has provided a consistent, qualitative picture of solvation. The significant influence of the solute on the dynamic properties of the water molecules is limited to a first solvation layer. Further, the influence of individual functional groups is localized. The solvent "structure" which is induced in the vicinity of nonpolar groups, and the concomitant configurational confinement of water molecules, is a result of the maintenance of bulk-like intermolecular hydrogen bonding within the constraint of a reduced number of neighbors capable of participating in the bonds. The nonpolar groups are incapable of forming hydrogen bonds and it is this property which distinguishes them from the polar groups. The decreased mobility of the solvent near nonpolar groups arises primarily from configurational (entropic) barriers rather than energetic barriers. Although certain geometrical aspects of the system are "clathrate-like", the term is misleading in its implications with respect to the number and strength of intermolecular bonds. The bulk-like dynamics observed for solvent near the solute polar groups is consistent with the interpretation that the polar groups interact with neighboring water molecules in approximately the same way as do other water molecules.

Additional details pertinent to this report are discussed elsewhere (7).

Abstract

The characteristics of water in the neighborhood of mixed-functional solutes containing both polar and nonpolar groups will be reviewed and illustrated by the detailed results obtained from a molecular dynamics simulation of a dilute aqueous solution of an alanine dipeptide. Both the solvent effect on the dipeptide and that of the dipeptide on the solvent will be described.

Literature Cited

1. Cooke, R.,; Kuntz, I.D. Annu. Rev. Biophys. Bioeng., 1974, 3, 95.
2. Rossky, P.J.; Karplus, M.; Rahman, A. Biopolymers, 1979, 18, 825.
3. Stillinger, F.H.; Rahman, A. J. Chem. Phys., 1974, 60, 1545.
4. Berne, B.J.; Pecora, R. "Dynamic Light Scattering", Wiley, New York, 1976.
5. Verlet, L. Phys. Rev., 1967, 159, 98; ibid, 1968, 165, 201; Rahman, A.; Stillinger, F.H. ibid, 1964, 136, A405.
6. Hertz, H.G. Prog. Nucl. Magn. Reson. Spectrosc., 1967, 3, 159.
7. Rossky, P.J.; Karplus, M. J. Am. Chem. Soc., 1979, 101, 1913.

RECEIVED January 4, 1980.